



This is a repository copy of *Model-free adaptive control for MEA-based post-combustion carbon capture processes*.

White Rose Research Online URL for this paper:
<http://eprints.whiterose.ac.uk/130219/>

Version: Accepted Version

Article:

Li, Z., Ding, Z., Wang, M. orcid.org/0000-0001-9752-270X et al. (1 more author) (2018) Model-free adaptive control for MEA-based post-combustion carbon capture processes. *Fuel*, 224. pp. 637-643. ISSN 0016-2361

<https://doi.org/10.1016/j.fuel.2018.03.096>

Reuse

This article is distributed under the terms of the Creative Commons Attribution-NonCommercial-NoDerivs (CC BY-NC-ND) licence. This licence only allows you to download this work and share it with others as long as you credit the authors, but you can't change the article in any way or use it commercially. More information and the full terms of the licence here: <https://creativecommons.org/licenses/>

Takedown

If you consider content in White Rose Research Online to be in breach of UK law, please notify us by emailing eprints@whiterose.ac.uk including the URL of the record and the reason for the withdrawal request.



eprints@whiterose.ac.uk
<https://eprints.whiterose.ac.uk/>

Model-free adaptive control for MEA-based post-combustion carbon capture processes

Ziang Li^a, Zhengtao Ding^{a,*}, Meihong Wang^b, Eni Oko^b

^a*School of Electrical and Electronic Engineering, University of Manchester, Manchester M13 9PL, UK*

^b*Department of Chemical and Biological Engineering, University of Sheffield, Sheffield S1 3JD, UK*

Abstract

For the flexible operation of mono-ethanol-amine-based post-combustion carbon capture processes, recent studies concentrate on model-based protocols which require underline model parameters of carbon capture processes for controller design. In this paper, a novel application of the model-free adaptive control algorithm is proposed that only uses measured input-output data for carbon capture processes. Compared with proportional-integral control, the stability of the closed-loop system can be easily guaranteed by increasing a stabilizing parameter. By updating the pseudo-partial derivative vector to estimate a dynamic model of the controlled plant on-line, this new protocol is robust to plant uncertainties. Compared with model predictive control, tuning tests of the protocol can be conducted on-line without non-trivial repetitive off-line sensitivity or identification tests. Performances of the model-free adaptive control are demonstrated within a neural-network carbon capture plant model, identified and validated with data generated by a first-principle carbon capture model.

Keywords: Post-combustion carbon capture, Process control, Model-free adaptive control, System identification, Neural networks

*Corresponding author. Tel: +44 1613 064663

Email address: zhengtao.ding@manchester.ac.uk (Zhengtao Ding)

1. Introduction

1.1. Background

Power generation from fossil fuel combustion is the single largest contributor of CO₂ emission [1]. The mono-ethanol-amine (MEA)-based post-combustion carbon capture (PCC) [2] technology is feasible for the large-scale CO₂ absorption since it can be achieved with relative simple retrofits of conventional fossil-fuel power plants [3]. To compensate load variations, for instance, due to intermittent renewable power sources, a fossil-fuel power plant usually supplies flexible power generation and sometimes serves as a swing generator for the power network. These inevitably cause fluctuations of the emitted flue gas flow rate and the mass fraction of CO₂ in the flue gas which are external disturbances [4] of the MEA-based PCC process and deteriorate model-based control performances. A control protocol for the process must be robust when confronting these uncertainties. Furthermore, for a tight CO₂ emission target [4] or a time-variant CO₂ allowance market condition [5], the plant controller should be appropriately designed such that the closed-loop system has fast responses.

1.2. Literature review

Previous studies of MEA-based PCC processes concentrated on proportional-integral (PI) control [4, 6, 7] with the relative gain array pairing strategy. Due to the optimality and flexibility requirements, recently, model predictive control (MPC) is implemented for the process [8, 9]. This model-based method is more appreciated since its optimality leads to fast responses or lower energy consumption according to a diverse range of the real-time objectives or scheduled load variations of a power plant. Although a dynamic PCC model [1] can be constructed in terms of the rigorous rate-based approach considering both chemical and physical properties, such a first-principle model is too

27 complicated for the model-based control [10, 11]. An identified model serving
28 as the underline model is imperative to reduce the model complexities while
29 ensure the model-based control performances. Previous studies focused on the
30 optimal operation of the model-based control such as MPC but paid little at-
31 tention to system identification before implementing such a control protocol.
32 On the other hand, when the PCC process operation is coupled with a power
33 plant [4], uncertain conditions of the power plant may degrade dynamic perfor-
34 mances of the carbon capture facilities. For instance, fluctuations of either the
35 flue gas flow rate or the CO₂ mass fraction in the flue gas, dependent on the
36 power plant load conditions, will change the operating point of the PCC pro-
37 cess. These disturbances cause extra mismatches between the model and the
38 controlled non-linear PCC plant, which is classified as model uncertainties. A
39 large number of sensitivity [6] or identification [12] tests for different operating
40 points of the controlled plant must be conducted before the controller can be
41 properly tuned and implemented on-line. It makes the model-based controller
42 design a non-trivial issue.

43 *1.3. Aim of the paper and its novelties*

44 In this paper, a novel model-free adaptive control (MFAC) protocol [13, 14]
45 is applied to a non-linear MEA-based PCC plant model identified based on a
46 validated neural network model using the validated data [15] generated by a first-
47 principle model. Compared with PI control using predefined tuning parameters
48 around fixed operating points, MFAC uses compact form dynamic linearisation
49 (CFDL) or partial form dynamic linearisation (PFDL) to form a time-variant
50 PCC model on-line, inferring that the model adapts to plant operating point
51 changes. Compared with the model-based protocol which requires non-trivial
52 sensitivity or identification tests to determine a model for off-line tuning before
53 on-line implementation, MFAC has a simpler tuning procedure. The identified

54 PCC model is only used for the initial off-line tuning. Thereafter, the tuning
55 parameters can be flexibly retuned on-line with the measured input-output data
56 of the controlled non-linear PCC plant. No model parameters identified off-line
57 are required on-line. The underline model parameters, however, are essential for
58 model-based protocols. They are used to ensure the stability and performances
59 of the closed-loop system, inferring a complex and repetitive off-line tuning pro-
60 cedure. PI control requires no underline model parameters same as MFAC, but
61 its stability analysis is based on models. MFAC can easily guarantee stability
62 by a stabilizing parameter.

63 *1.4. Outline of the paper*

64 This paper is organized as follows. Firstly, the system identification problem
65 is discussed to build a validated non-linear PCC model with a neural network
66 structure using the data generated by a first-principle model. Secondly, com-
67 pared with generalized predictive control (GPC), MFAC is designed based on
68 an iterative algorithm including on-line linear model update, control policy up-
69 date and a reset rule. Thirdly, with the identified PCC model serving as the
70 controlled non-linear plant, simulation results of MFAC are presented compared
71 with PI control and GPC. Conclusions are given in the end.

72 **2. Model development**

73 *2.1. Dynamic modelling of the post-combustion carbon capture process*

74 The first-principle dynamic model of the PCC process **in this paper has**
75 **been** developed in gPROMS[®] with the rate-based approach **using the design**
76 **and operation specifications in [17]**. All the reactions in PCC are assumed
77 to attain equilibrium. Validation of this model was made using data of pilot
78 plants [4, 15]. The flow diagram (Fig. 1) shows the flue gas is initially fed into
79 the **bottom of the absorber while the lean MEA solution is injected from the**

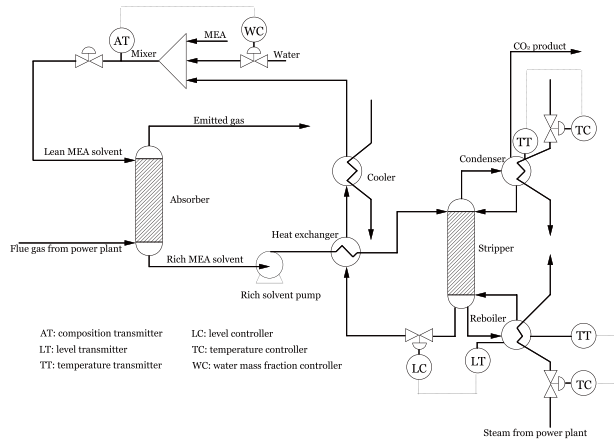


Fig. 1. The process flow diagram of a PCC plant [16, 17].

80 top. After chemical reactions between CO_2 and the lean MEA countercurrently
 81 in the column, the purified gas with less CO_2 is vented to the atmosphere while
 82 a carbon-rich MEA solution is pumped into the downstream lean/rich cross heat
 83 exchanger and exchanges energy with the lean solution from the stripper. The
 84 stripper has the analogous structure as the absorbers. The pre-heated rich MEA
 85 from the exchanger outlet is pumped to the upper-stage and heated up when
 86 flowing down through the column. The heat is provided via a reboiler which
 87 separates CO_2 from the rich MEA and reproduces the lean MEA to process
 88 the consecutively discharged flue gas. Although a rigorous model can be built
 89 considering chemical reactions, it is too complex for control design [10]. A
 90 feasible mathematical model must be identified [8].

91 2.2. Identification of neural networks for dynamic carbon capture processes

92 For the PCC process which is complex and non-linear, neural networks
 93 [18, 19] can be selected to identify mathematical models based on off-line data
 94 generated by the above first-principle model. Note that the tracking problem
 95 of the carbon capture level is primarily considered in Section 3. For brevity,
 96 the lean loading and the re-boiler temperature are assumed to be fixed around

97 0.28 mol/mol and 387 K, respectively, for all cases in the later simulations. On
 98 that basis, a model related to the carbon capture level dynamics is built with
 99 three inputs and one output. The three inputs are the flue gas flow rate (kg/s),
 100 $d_1(t)$, mass fraction of CO₂ in the flue gas, $d_2(t)$ and the lean MEA flow rate
 101 (kg/s), $u(t)$, respectively. The output is the CO₂ or carbon capture level (%),
 102 denoted by $y(t)$. The candidate models of this process are neural networks with
 103 one hidden layer. Referring to Fig. 2, the model structure is represented by

$$\hat{y}(t+1) = \mathbf{w}^T \mathbf{z}(\mathbf{x}(t)) + b_o \quad (1)$$

104 where $\hat{y}(t+1)$ is the estimated capture level of the carbon capture process at
 105 time $t+1$; $\mathbf{w} = (w_1, w_2, \dots, w_H)^T \in \mathbb{R}^H$ and $b_o \in \mathbb{R}$ are the weight vector and
 106 the bias, respectively, between the hidden and output layers; and $\mathbf{x}(t) \in \mathbb{R}^n$ is
 107 the input features at time t and defined as $\mathbf{x}(t) \triangleq (x_1(t), x_2(t), \dots, x_n(t))^T =$
 108 $(y(t), y(t-1), \dots, y(t-n_a+1), d_1(t), d_1(t-1), \dots, d_1(t-n_{d1}+1), d_2(t), d_2(t-$
 109 $1), \dots, d_2(t-n_{d2}+1), u(t), u(t-1), \dots, u(t-n_b+1))^T$ with $n = n_a + n_b +$
 110 $n_{d1} + n_{d2}$. n_a , n_b , n_{d1} , and n_{d2} are model orders which must be determined
 111 in terms of model performances. $\mathbf{z}(\mathbf{x})$ is the output of the hidden layer, i.e.,
 112 $\mathbf{z}(\mathbf{x}) \triangleq (z_1, z_2, \dots, z_H)^T = g(\mathbf{V}\mathbf{x} + \mathbf{b}) \in \mathbb{R}^H$ with $g(\cdot)$ being an element-wise
 113 activation function for each entry of $\mathbf{V}\mathbf{x} + \mathbf{b}$ where $\mathbf{V} \in \mathbb{R}^{H \times n}$ and $\mathbf{b} \in \mathbb{R}^H$
 114 are the weight matrix and the bias vector, respectively, between the input layer
 115 and hidden layer. Without losing generality, for $h \in \mathbb{R}$, the scalar activation
 116 function is logistic, i.e., $g(h) = 1/(1 + \exp(-h))$. **For a specific candidate model**
 117 **based on neural networks, the model parameters are weights (\mathbf{w} , \mathbf{V}) and biases**
 118 **(b_o , \mathbf{b}) which should be identified using the input and output data from the first-**
 119 **principle model. The total number of model parameters including weights and**
 120 **biases for the above neural network is $D = [(n+2) \cdot H] + 1$. To avoid overfitting**
 121 **[20], for two candidate models with similar model validation performances, the**

122 model with less complexity, i.e., smaller D , is preferred.

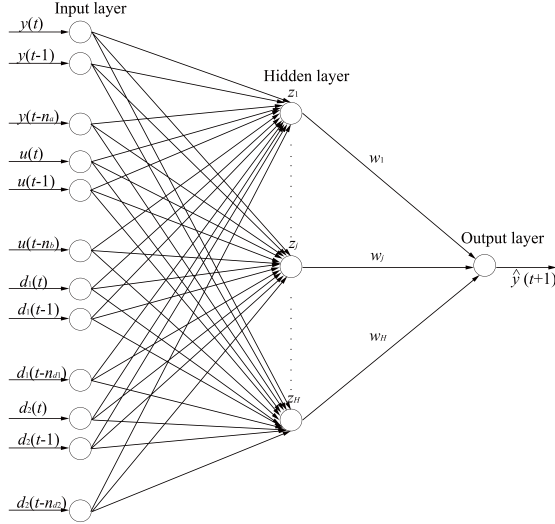


Fig. 2. A multi-input-single-output neural network with one hidden layer.

123 *2.3. Model order selection with AIC*

124 Akaike's information criterion (AIC) is used to determine the number of
 125 model parameters D_0 . For a candidate model, i.e., the model structure (Eq. (1))
 126 with a specific hidden layer size H and model orders, the residual is defined as
 127 the difference between the observation and the one-step-ahead prediction of
 128 the output, which is $\epsilon(t) = y(t) - \hat{y}(t)$. $y(t)$ is the observed capture level of
 129 PCC processes. On that basis, the AIC value is estimated by $\text{AIC} = \ln(\hat{\sigma}^2) +$
 130 $2D_0/N$ with $\hat{\sigma}^2 = (1/N) \sum_{t=1}^N \epsilon(t)^2$ where $\hat{\sigma}$ is an estimate of the noise standard
 131 deviation σ ; N is the number of data samples; and $D_0 = D + 1$ is the number of
 132 model parameters including σ . In practice, the model orders may not be exactly
 133 selected by AIC. Residual analysis is used to validate the candidate models.

134 *2.4. Residual analysis*

135 The residual analysis [12] suggests a validated model has residuals $\epsilon(t)$
 136 which are serially independent and unrelated to past inputs. Two correlation-

137 based intermediate variables are defined as $\hat{R}_\epsilon^N(\tau) = (1/N) \sum_{t=1}^N \epsilon(t)\epsilon(t-\tau)$
138 and $\hat{R}_{\epsilon u}^N(\tau) = (1/N) \sum_{t=1}^N \epsilon(t)u(t-\tau)$. $\zeta_1(\tau)$ and $\zeta_2(\tau)$ are then defined as
139 $\hat{\zeta}_1(\tau) = (N/\hat{\sigma}^4) \cdot (\hat{R}_\epsilon^N(\tau))^2 \sim \chi^2(1)$ and $\hat{\zeta}_2(\tau) = \sqrt{N/\hat{\sigma}^2 P(\tau)} \hat{R}_{\epsilon u}^N(\tau) \sim \mathcal{N}(0, 1)$
140 with $P(\tau) = (1/N) \sum_{t=1}^N u(t-\tau)^2$. For a validated model, $\zeta_1(\tau)$ and $\zeta_2(\tau)$ should
141 be within the α -level confidence intervals determined by the chi-squared- and
142 normally-distributed random variables, respectively.

143 3. Model-based and model-free control protocols

144 The tracking problem of the carbon capture level $y(t)$ for the controlled
145 non-linear PCC plant is considered in this section. The manipulated input is
146 the lean MEA flow rate $u(t)$ [4, 6]. The disturbances are the flue gas flow rate
147 (kg/s) $d_1(t)$ and the mass fraction of CO₂ in the flue gas $d_2(t)$. Two possible
148 protocols are discussed. One is model-based, called GPC; the other is MFAC.
149 MFAC should be more favourable since it can be implemented easily on-line
150 without models identified off-line.

151 3.1. Generalized predictive control

152 The advanced model-based protocol called GPC is briefly introduced, which
153 requires an underline model (i.e., a prediction model) of the controlled plant

$$A(q^{-1})y(t+1) = B(q^{-1})u(t) + L(q^{-1})\mathbf{d}(t) + \frac{e(t+1)}{\Delta} \quad (2)$$

154 where $\mathbf{d}(t) \triangleq (d_1(t), d_2(t))^T$, $A(q^{-1}) = 1 + a_1q^{-1} + a_2q^{-2} + \dots + a_{n_a}q^{-n_a}$,
155 $B(q^{-1}) = b_0 + b_1q^{-1} + b_2q^{-2} + \dots + b_{n_b-1}q^{-n_b+1}$, $L(q^{-1}) = \mathbf{l}_0 + \mathbf{l}_1q^{-1} + \mathbf{l}_2q^{-2} +$
156 $\dots + \mathbf{l}_{n_l-1}q^{-n_l+1}$, $\Delta = 1 - q^{-1}$, and $\mathbf{l}_i \in \mathbb{R}^{1 \times 2}$. The control objective is defined
157 as

$$J = (\mathbf{r} - \mathbf{y})^T \mathbf{Q}(\mathbf{r} - \mathbf{y}) + \mathbf{u}^T \mathbf{R} \mathbf{u} \quad (3)$$

158 where $\mathbf{Q} \in \mathbb{R}^{N_r \times N_r}$, $\mathbf{R} \in \mathbb{R}^{N_r \times N_r}$, $\mathbf{r} = (r(t+1), r(t+2), \dots, r(t+N_r))^T$, $\mathbf{y} =$
159 $(\hat{y}(t+1), \hat{y}(t+2), \dots, \hat{y}(t+N_r))^T$, $\mathbf{u} = (\Delta u(t), \Delta u(t+1), \dots, \Delta u(t+N_r-1))^T$,
160 and $\mathbf{d} = (\mathbf{d}(t)^T, \mathbf{d}(t+1)^T, \dots, \mathbf{d}(t+N_r-1)^T)^T$. Using Diophantine equation
161 [21] iterations, the objective is rewritten as $J = (\mathbf{G}\mathbf{u} + \mathbf{f}' - \mathbf{r})^T \mathbf{Q}(\mathbf{G}\mathbf{u} + \mathbf{f}' - \mathbf{r}) +$
162 $\mathbf{u}^T \mathbf{R}\mathbf{u}$ where \mathbf{f}' is the filtered responses [21]. The control policy is then derived
163 as

$$\mathbf{u} = (\mathbf{G}^T \mathbf{Q} \mathbf{G} + \mathbf{R})^{-1} \mathbf{G}^T \mathbf{Q} (\mathbf{r} - \mathbf{f}') \quad (4)$$

164 where only the first row of \mathbf{u} is implemented for the controlled plant. **Note that**
165 **for a model-based protocol, the underline model parameters from sensitivity or**
166 **identification tests are usually required. For this specific GPC algorithm, the**
167 **model parameters are $A(q^{-1})$, $B(q^{-1})$ and $L(q^{-1})$ which approximate the PCC**
168 **plant in some standard mathematical form (Eq. (2)). These model parameters**
169 **are the indispensable priori knowledge for the model-based control design. To**
170 **implement the control policy (Eq. (4)), both the matrix \mathbf{G} and the filter \mathbf{f}'**
171 **should be determined by $A(q^{-1})$, $B(q^{-1})$ and $L(q^{-1})$ beforehand, which infers**
172 **that GPC is model-based.**

173 3.2. Model-free adaptive control

174 The PCC process is commonly modelled by first-principle strategies such as
175 equilibrium-based or rate-based approaches [3], which infers that the process
176 involves non-linearities. Note that the time-variant flue gas flow rate, $d_1(t)$ and
177 the mass fraction of CO_2 in flue gas, $d_2(t)$ may cause variations of the process
178 operating point. Thus, non-linearities will lead to mismatches between the
179 controlled plant and the underline model of the model-based controllers, such
180 as GPC. The model-free protocol [14] can form a dynamic linear model on-
181 line for the controlled non-linear plant with a pseudo-partial derivative (PPD)

182 vector $\Phi(t)$. No off-line model parameters are required when the controller is
 183 implemented in real time. As the process operating point varies, $\Phi(t)$ adapts to
 184 the changes. The control method with $\Phi(t)$ is termed as PFDL which describes
 185 the relationship between the input and the output with

$$\Delta y(t+1) = \Phi(t)\Delta \mathbf{U}(t) \quad (5)$$

186 where $\Phi(t) = (\phi_1(t), \phi_2(t), \dots, \phi_L(t)) \in \mathbb{R}^{1 \times L}$ and $\Delta \mathbf{U}(t) = (\Delta u(t), \Delta u(t-1), \dots, \Delta u(t-L+1))^T \in \mathbb{R}^L$. $u(t)$, the lean MEA flow rate, is the manipulated
 187 input while $y(t)$, the capture level, is the controlled output. When $L = 1$, Eq. (5)
 188 is reduced to the CFDL-based description. True $\Phi(t)$ can be estimated by $\hat{\Phi}(t)$
 189 based on the optimisation problem of $J_\Phi = (1/2)\|\hat{\Phi}(t) - \hat{\Phi}(t-1)\|^2$ subject to
 190 $\Delta y(t) = \hat{\Phi}(t)\Delta \mathbf{U}(t-1)$ which can be solved by the modified projection algorithm
 191 [14]. A control objective is defined as $J_U = \|r(t+1) - y(t+1)\|^2 + \lambda\|\Delta \mathbf{U}(t)\|^2$.
 192 By minimizing both J_Φ and J_U , the on-line model update is
 193

$$\begin{aligned} \hat{\Phi}(t) = & \hat{\Phi}(t-1) \\ & + \frac{\eta(\Delta y(t) - \hat{\Phi}(t-1)\Delta \mathbf{U}(t-1))\Delta \mathbf{U}^T(t-1)}{\mu + \|\Delta \mathbf{U}(t-1)\|^2} \end{aligned} \quad (6)$$

194 and the control policy update is

$$\begin{aligned} u(t) = & u(t-1) + \frac{\rho_1 \hat{\phi}_1(t)(r(t+1) - y(t))}{\lambda + |\hat{\phi}_1(t)|^2} \\ & - \frac{\hat{\phi}_1(t) \sum_{m=2}^L \rho_m \hat{\phi}_m(t) \Delta u(t-m+1)}{\lambda + |\hat{\phi}_1(t)|^2} \end{aligned} \quad (7)$$

195 where $\hat{\Phi}(t) = (\hat{\phi}_1(t), \hat{\phi}_2(t), \dots, \hat{\phi}_L(t)) \in \mathbb{R}^{1 \times L}$ and $r(t+1)$ is the set-point of
 196 the output. For stability of the closed-loop system, the reset rule is

$$\begin{aligned} \hat{\phi}_1(t) = \hat{\phi}_1(1), \text{ if } |\hat{\phi}_1(t)| < b \text{ or } |\hat{\phi}_1(t)| > \alpha b \\ \text{or } \text{sign}(\hat{\phi}_1(t)) \neq \text{sign}(\hat{\phi}_1(1)). \end{aligned} \quad (8)$$

197 Eqs. (6), (7) and (8) form the iterative algorithm of the MFAC protocol [13].
 198 To apply this algorithm, tuning parameters within constraints (i.e., $\eta \in (0, 1)$,
 199 $\mu > 0$, $\boldsymbol{\rho} = (\rho_1, \rho_2, \dots, \rho_L)^T$ with $\rho_m \in (0, 1)$ for any m , $\lambda > \lambda_{\min} > 0$,
 200 $\alpha > 1$, and $b > 0$) should be determined by the user. η and μ are related to
 201 the adaptive performances of the dynamic linear model for the controlled PCC
 202 plant. $\boldsymbol{\rho}$ and λ are related to the control performances for the plant. For fast
 203 responses, η and $\boldsymbol{\rho}$ should be increased while for smooth dynamics, μ and λ
 204 should be increased. The PPD vector $\hat{\Phi}(t)$ is updated on-line without using any
 205 prior knowledge of the off-line model, which implies the iterative algorithm is
 206 model-free. Arbitrary initial conditions of $\hat{\Phi}(t=1)$ should be specified to set
 207 up the iteration.

208 Compared with PI control, the above iterative method is easy to guarantee
 209 stability. If the closed-loop system is unstable or marginally stable, only the
 210 stabilizing parameter λ should be increased for the stabilization while PI control
 211 requires stability analysis such as the Nyquist criterion to determine whether
 212 to increase or decrease tuning parameters. In addition, the Nyquist criterion is
 213 a model-based method requiring model parameters. Furthermore, PI control is
 214 generally designed around fixed operating points while MFAC forms an adaptive
 215 dynamic linear model using on-line model update (Eq. (6)), i.e., MFAC already
 216 considers model uncertainties and should have strong robustness.

217 Compared with GPC requiring a prediction model, MFAC can be easily
 218 tuned on-line with measured input-output data of the controlled plant. If the

219 underline model is inaccurate, the performances of GPC will be deteriorated.
220 For the PCC process which is sensitive to ambient environments and is non-
221 linear, a large number of sensitivity or identification tests should be conducted
222 around different operating points of the controlled plant before the controller can
223 be applied on-line. MFAC only uses input-output data of the PCC plant. No
224 off-line model parameters are necessary for the on-line control implementation.
225 The identified mathematical model of the PCC process is only used for the
226 initial off-line tuning. Afterwards, if the control performance is unsatisfactory,
227 MFAC can be retuned on-line [13] without off-line models. However, if the
228 control performance of a model-based controller is poor, the model may be
229 re-identified off-line based on new data generated by the first-principle model,
230 which is non-trivial. Therefore, the implementation of MFAC is easier.

231 4. Simulation results

232 4.1. Identification of a carbon capture plant model with neural networks

233 The observed data for the plant model identification are generated by the
234 first-principle PCC model [17] with the sampling time $T_s = 2.5$ s. During
235 preprocessing, dc-offsets of both the input features $\mathbf{x}(t)$ and output $y(t)$ are
236 removed. The model structure is a neural network with an unknown hidden
237 layer size and model orders, both reflected by D_0 , the total number of model
238 parameters. In Section 2, D_0 is determined by n_a , n_b , n_{d1} , n_{d2} and H . To
239 reduce the number of candidate models, $n_b = n_{d1} = n_{d2}$ with the hidden layer
240 size $H = 1$ is assumed for the initial model order selection. Only n_a and
241 n_b should be determined to fix D_0 . For both n_a and n_b ranging from 1 to
242 10, the model performances are quantized by AIC. Theoretically, the selected
243 model orders should have the minimum AIC value (Fig. 3a), i.e., $n_a = 10$ and
244 $n_b = 5$. The model order pair selected by Akaike's information criterion with a

245 correction for finite sample sizes (AIC_c) or Bayesian information criterion (BIC)
 246 [20] is $n_a = 5$ and $n_b = 5$.

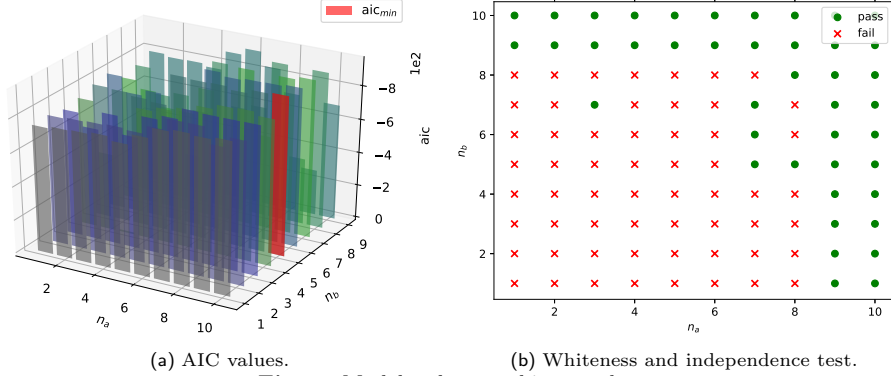


Fig. 3. Model order searching results.

247 Correspondingly, the selected candidate models must pass the whiteness and
 248 independence tests so as to validate their performances **on approximating the**
 249 **first principle PCC model [17]**. The tests are conducted not only for the models
 250 selected by AIC, AIC_c or BIC, but the candidate models with orders around
 251 the neighbours of the criterion-based ones, i.e., n_a and n_b are searched within
 252 $\{1, 2, 3, 4, 5, 6, 7, 8, 9, 10\}$. The hidden layer size H is enumerated from 1 to
 253 10. For each specified H and n_a - n_b pair, a validated model must meet two
 254 constraints: (a) It can achieve a good fit (over 90% fit) with the observed data
 255 generated by the first-principle model; (b) the residual $\epsilon(t)$ of the candidate
 256 model can pass whiteness and independence tests. If there exists any H such
 257 that the whiteness and independence tests are passed, this n_a - n_b pair is recorded
 258 with “pass” (Fig. 3b). Although the model order pair, $n_a = 5$ and $n_b = 5$, is
 259 selected by AIC_c or BIC, the corresponding candidate model fails the tests
 260 (Fig. 3b). Table 1 only gives the smallest hidden layer sizes H_{\min} with respect
 261 to some typical model order pairs (determined by AIC, AIC_c , BIC, etc.) such
 262 that the candidate models can pass the whiteness and independence tests. It is
 263 observed that if the model has passed the tests, the fit percentage is generally

264 over 90%. Instead of the above constraints for validated models, the number of
 265 model parameters D_0 is further considered to avoid over-fitting. A candidate
 266 model with $n_a = 10$, $n_b = 1$, and $H_{\min} = 1$ is finally selected since $D_0 =$
 267 $(n + 2) \cdot H + 2 = 17$ is the smallest among all the validated models. According
 268 to input and output dynamics (Fig. 4) of the selected model, its fit percentage
 269 is 98.41% for the one-step-ahead prediction. In addition, the fit percentage of
 270 the multi-step-ahead prediction for the carbon capture level is 93.43%. This
 271 value is lower than 98.41% of the one-step-ahead prediction but still exceeds
 272 90%. The residual analysis (Fig. 5) of the model indicates $\zeta_1(\tau)$ and $\zeta_2(\tau)$ are
 273 within the 99% confidence intervals.

Table 1
Validated model orders and fit percentages.

(n_a, n_b)	H_{\min}	fit (%)
(5, 5)	/	/
(7, 5)	3	97.77
(10, 1)	1	98.41
(10, 5)	1	98.42

Table 2
Controller design.

	PI		CFDL-MFAC	PFDL-MFAC
K_p	0.01	μ	0.002	0.002
K_i	0.017	λ	25	40
		ρ	(1)	(0.8, 0.05, 0.001) ^T
		α	200	200
		η	0.4	0.4
		b	0.1	0.1
		L	1	3
		$\hat{\Phi}(1)$	(3)	(3, -5, -2)

274 4.2. Model-free adaptive controller design

275 The performances of CFDL- and PFDL-MFAC are evaluated based on the
 276 previous validated non-linear PCC plant model, i.e., the controlled plant in the

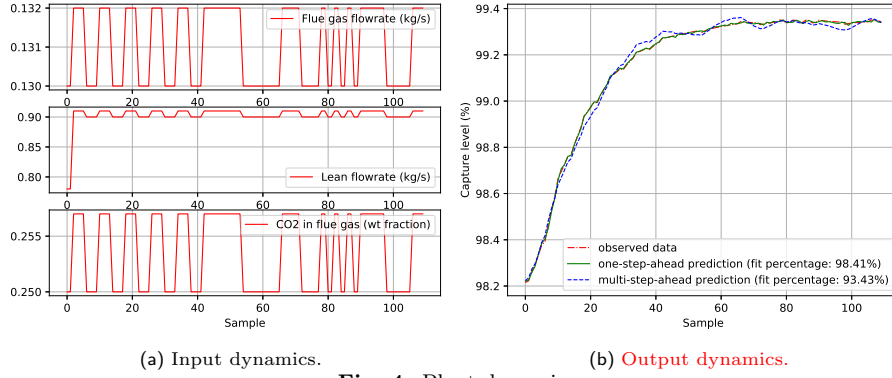


Fig. 4. Plant dynamics.

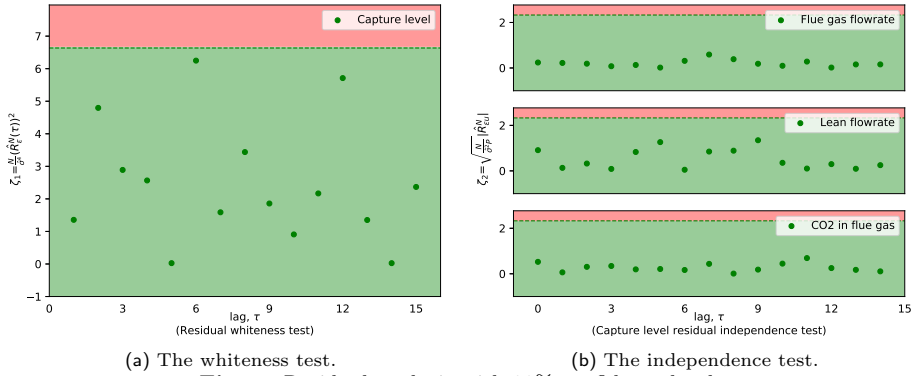
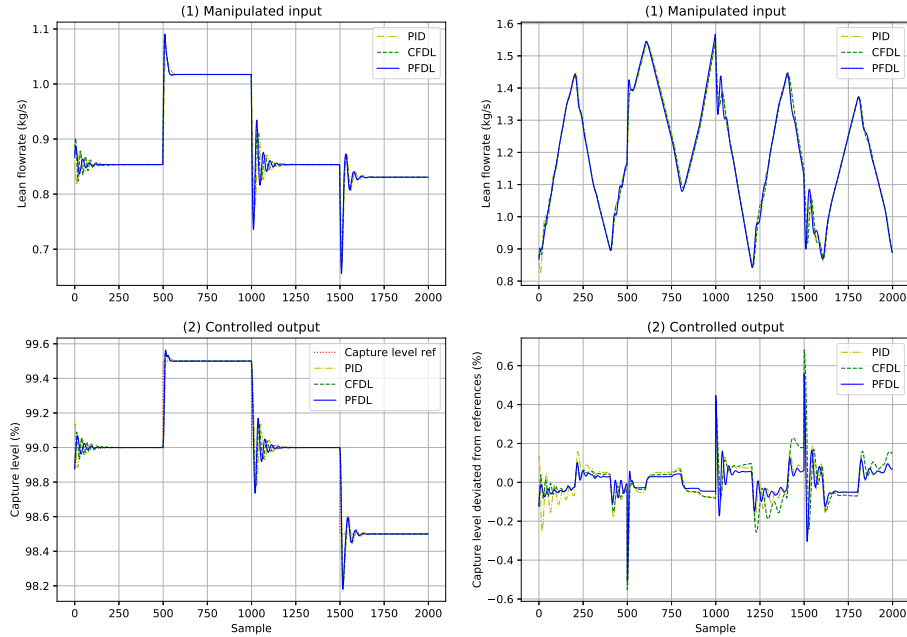


Fig. 5. Residual analysis with 99% confidence level.

277 subsequent sections. PI control results are also given for comparisons. The
 278 lean MEA flow rate is the manipulated input while the carbon capture level is
 279 the controlled output. The original controlled plant is supposed to be free of
 280 disturbances. During the tuning process, K_p and K_i (Table 2) of PI control [17]
 281 are tuned to ensure tracking performances of the capture level as best as possible.
 282 Then, instead of PI control, MFAC can be tuned as discussed in Subsection 3.2
 283 and implemented to achieve similar performances (Fig. 6a) with the designed
 284 tuning parameters (Table 2). Although the number of tuning parameters for
 285 MFAC is larger than that for PI control, MFAC is easy to ensure stability [14].
 286 PI control needs extra stability analysis of the closed-loop system.

287 Afterwards, the time-variant disturbances, i.e., the flue gas flow rate and the



(a) The undisturbed closed-loop system. (b) The disturbed closed-loop system.
Fig. 6. MFAC and PI control results.

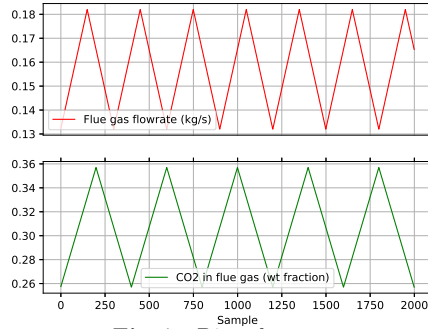
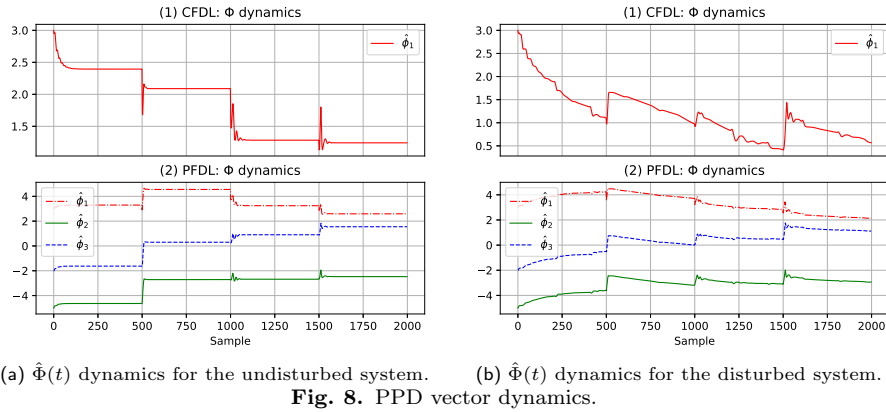


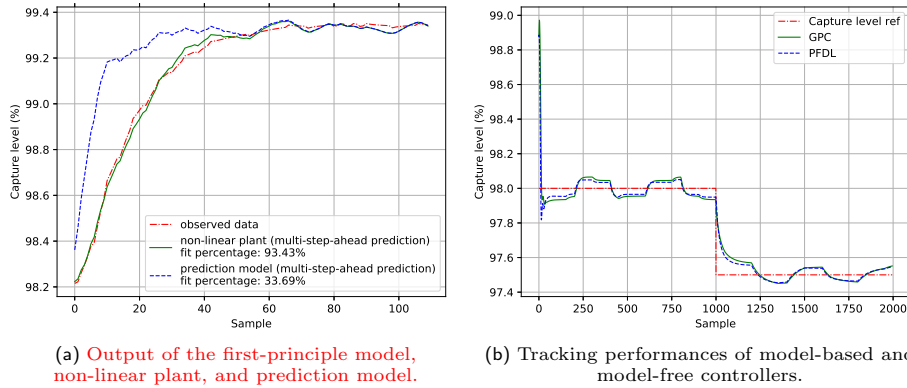
Fig. 7. Disturbances.

288 CO₂ mass fraction of the flue gas (Fig. 7), are applied to the controlled non-linear
 289 PCC plant, which can be periodical ramp changes due to the variations of power
 290 generation [4]. Simultaneously, the reference signal of the carbon capture level
 291 is generated identically to the one of the undisturbed system (Fig. 6a). Based
 292 on the previous tuning parameters (Table 2), only the capture level deviations
 293 from the references (Fig. 6b) are plotted, where PFDL-MFAC has the smoothest

294 transient responses of the output, i.e. the smallest carbon capture level devia-
 295 tions than the PI control and CFDL-MFAC algorithms. PFDL-MFAC is better
 296 (Fig. 6b) than CFDL, since time-variant PPD $\hat{\Phi}(t)$ of PFDL with a longer length
 297 $L = 3$ (Table 2) adaptively catches more system dynamics. CFDL-MFAC with
 298 fewer tuning parameters than PFDL-MFAC, however, can be designed more
 299 easily for simple plants [14]. Both CFDL- and PFDL-MFAC can guarantee sta-
 300 bility by increasing the stabilizing parameter λ . Time-variant $\hat{\Phi}(t)$ for CFDL
 301 and PFDL (Fig. 8) dynamically estimate the controlled non-linear plant.



302 **4.3. Comparison between model-based and model-free controllers**



303 PFDL-MFAC is compared with GPC in this subsection. Note that the con-
 304 trolled non-linear PCC plant is the validated neural network selected in Subsec-
 305 tion 4.1. The prediction model (Eq. (2)) is linearised based on this non-linear
 306 plant using the first-order Taylor approximation so as to derive $A(q^{-1})$, $B(q^{-1})$
 307 and $D(q^{-1})$. These polynomials inevitably generate model uncertainties due
 308 to plant non-linearities. There exist mismatches between the output responses
 309 of the prediction model, the controlled non-linear plant and the first-principle
 310 model (Fig. 9a). Based on the prediction model, to implement the GPC algo-
 311 rithm, the time horizon N_r , and the weight matrices \mathbf{Q} and \mathbf{R} in the control
 312 objective (Eq. (3)) should be determined by the user. N_r is the concerned time
 313 horizon. \mathbf{Q} is the penalty of the tracking error (i.e., $r(t+k) - y(t+k)$) within
 314 the time horizon N_r . \mathbf{R} is the penalty of the manipulated input deviation (i.e.,
 315 $\Delta u(t+k) = u(t+k) - u(t+k-1)$) within the time horizon N_r . The control
 316 objective (Eq. (3)) indicates there should be trade-off between the tracking er-
 317 ror and the input manipulation. For the smooth input dynamics, entries of \mathbf{Q}
 318 should be large while those of \mathbf{R} should be small. In contrast, for the fast output
 319 responses, entries of \mathbf{Q} should be small while those of \mathbf{R} should be large. In this
 320 case study, the best performance of GPC is obtained with the tuning paramete-
 321 rs of $N_r = 3$, $\mathbf{Q} = 1 \cdot I_{N_r \times N_r}$ and $\mathbf{R} = 30 \cdot I_{N_r \times N_r}$ where $I_{N_r \times N_r} \in \mathbb{R}^{N_r \times N_r}$
 322 is an identity matrix. Simultaneously, Fig. 9b shows PFDL-MFAC achieves a
 323 similar tracking performance as GPC. Nevertheless, an underline model should
 324 be identified before the tuning parameters of GPC can be tested on-line. The
 325 model not only lacks non-linearities of the controlled plant but is usually ob-
 326 tained with off-line sensitivity or identification tests. Both of them make the
 327 tuning procedure more complex than MFAC.

328 **5. Conclusions**

329 We have identified a validated non-linear PCC plant model using the data
330 generated by a first-principle model. The candidate models are approximately
331 located by model order selection criteria such as AIC, AIC_c and BIC, and then
332 searched around the neighbours of the criterion-determined model orders. The
333 plant model can pass residual analysis and fit well with the data set.

334 We have implemented the PI control and the model-free algorithms, namely,
335 CFDL- or PFDL-MFAC within the validated non-linear PCC plant model.
336 PFDL-MFAC has shown the best performance when confronting model uncer-
337 tainties caused by time-variant disturbances. CFDL-MFAC, however, can be
338 tuned easily since it has fewer tuning parameters. Both CFDL- and PFDL-
339 MFAC can guarantee the stability of the closed-loop system by the stabilizing
340 parameter λ , easier than PI control using the model-based Nyquist criterion.

341 We have compared PFDL-MFAC with a model-based method called GPC.
342 PFDL-MFAC can be more flexibly tuned on-line without model parameters
343 determined during the off-line system identification. GPC, however, must be
344 applied based on underline models, which is linearised around specified equilib-
345 rium points of the controlled non-linear plant. Extra time should be taken to
346 ensure the model performances. When performances of such a model-based con-
347 troller are unsatisfactory, re-identification of underline models may be required,
348 which is non-trivial. Consequently, PFDL-MFAC can be flexibly designed and
349 implemented easily on-line with a simplified off-line tuning process.

350 **Declaration of interest**

351 None.

352 **References**

- 353 [1] Lawal A, Wang M, Stephenson P, Yeung H. Dynamic modelling of CO₂
354 absorption for post combustion capture in coal-fired power plants. *Fuel*
355 2009;88(12):2455–62.
- 356 [2] Bui M, Gunawan I, Verheyen V, Feron P, Meuleman E, Adeloju S. Dynamic
357 modelling and optimisation of flexible operation in post-combustion CO₂
358 capture plants-A review. *Computers & Chemical Engineering* 2014;61(Sup-
359 plement C):245–65.
- 360 [3] Wang M, Lawal A, Stephenson P, Sidders J, Ramshaw C. Post-combustion
361 CO₂ capture with chemical absorption: A state-of-the-art review. *Chemical*
362 *Engineering Research and Design* 2011;89(9):1609–24.
- 363 [4] Lawal A, Wang M, Stephenson P, Obi O. Demonstrating full-scale post-
364 combustion CO₂ capture for coal-fired power plants through dynamic mod-
365 elling and simulation. *Fuel* 2012;101(Supplement C):115–28.
- 366 [5] Li Z, Ding Z, Wang M. Operation and bidding strategies of power plants
367 with carbon capture. *IFAC-PapersOnLine* 2017;50(1):3244–9. 20th IFAC
368 World Congress.
- 369 [6] Nittaya T, Douglas PL, Croiset E, Ricardez-Sandoval LA. Dynamic mod-
370 elling and control of MEA absorption processes for CO₂ capture from
371 power plants. *Fuel* 2014;116(Supplement C):672–91.
- 372 [7] Lin YJ, Wong DSH, Jang SS, Ou JJ. Control strategies for flexi-
373 ble operation of power plant with CO₂ capture plant. *AIChE Journal*
374 2012;58(9):2697–704.
- 375 [8] Arce A, Mac Dowell N, Shah N, Vega LF. Flexible operation of solvent
376 regeneration systems for CO₂ capture processes using advanced control

- 377 techniques: Towards operational cost minimisation. *International Journal*
378 *of Greenhouse Gas Control* 2012;11(Complete):236–50.
- 379 [9] Sahraei MH, Ricardez-Sandoval L. Controllability and optimal schedul-
380 ing of a CO₂ capture plant using model predictive control. *International*
381 *Journal of Greenhouse Gas Control* 2014;30(Supplement C):58–71.
- 382 [10] Peng J, Edgar TF, Eldridge RB. Dynamic rate-based and equilibrium
383 models for a packed reactive distillation column. *Chemical Engineering*
384 *Science* 2003;58(12):2671–80.
- 385 [11] Hou ZS, Wang Z. From model-based control to data-driven control: Survey,
386 classification and perspective. *Information Sciences* 2013;235:3–35.
- 387 [12] Ljung L. *System Identification: Theory for the user*. PTR Prentice Hall
388 *Information and System Sciences Series*; 1987.
- 389 [13] Hou Z, Jin S. Data-driven model-free adaptive control for a class of MIMO
390 nonlinear discrete-time systems. *IEEE Transactions on Neural Networks*
391 2011;22(12):2173–88.
- 392 [14] Hou Z, Jin S. A novel data-driven control approach for a class of discrete-
393 time nonlinear systems. *IEEE Transactions on Control Systems Technology*
394 2011;19(6):1549–58.
- 395 [15] Dugas RE. Pilot plant study of carbon dioxide capture by aqueous mo-
396 noethanolamine. Ph.D. thesis; 2006.
- 397 [16] Li Z, Ding Z, Wang M. Optimal bidding and operation of a power plant with
398 solvent-based carbon capture under a CO₂ allowance market: A solution
399 with a reinforcement learning-based sarsa temporal-difference algorithm.
400 *Engineering* 2017;3(2):257–65.

- 401 [17] Biliyok C, Lawal A, Wang M, Seibert F. Dynamic modelling, validation
402 and analysis of post-combustion chemical absorption CO₂ capture plant.
403 International Journal of Greenhouse Gas Control 2012;9:428–45.
- 404 [18] Sipcz N, Tobiesen FA, Assadi M. The use of artificial neural network models
405 for CO₂ capture plants. Applied Energy 2011;88(7):2368–76.
- 406 [19] Li F, Zhang J, Oko E, Wang M. Modelling of a post-combustion CO₂
407 capture process using neural networks. Fuel 2015;151(Supplement C):156–
408 63.
- 409 [20] Burnham KP, Anderson DR. Model selection and multimodel inference:
410 a practical information-theoretic approach. Springer Science & Business
411 Media; 2002.
- 412 [21] Camacho EF, Alba CB. Model predictive control. Springer Science &
413 Business Media; 2013.